Targeting the efficacy of a dendrimer-based nanotherapeutic in heterogeneous xenograft tumors *in vivo*

Andrzej Myc, Jolanta Kukowska-Latallo, Peter Cao, Ben Swanson, Julianna Battista, Thomas Dunham and James R. Baker Jr

Our earlier studies have shown the *in vitro* and *in vivo* targeting of a generation 5 (G5) dendrimer-based multifunctional conjugate that contained folic acid (FA) as the targeting agent and methotrexate (MTX) as the chemotherapeutic drug. To clinically apply the synthesized G5-FA-MTX nanotherapeutic, it is important that the anticancer conjugate elicits cytotoxicity specifically and consistently. Toward this objective, we evaluated the large-scale synthesis of a G5-FA-MTX conjugate (Lot # 123–34) for its cytotoxic potential and specificity *in vitro* and *in vivo*. The cytotoxicity and specificity were tested by using a coculture assay in which FA receptor-expressing and nonexpressing cells (KB and SK-BR-3 cells, respectively) were cultured together and preferential killing was examined. The in-vitro data were compared with the in-vivo data obtained from a heterogeneous xenograft tumor model. The animal model of the artificial heterogeneous xenograft tumor showed that the nanotherapeutic was preferentially cytotoxic to KB cells. *Anti-Cancer Drugs* 21:186–192 © 2010 Wolters Kluwer Health | Lippincott Williams & Wilkins.

Anti-Cancer Drugs 2010, **21**:186–192

Keywords: coculture assay, dendrimer, heterogeneous xenograft tumor model, methotrexate, neoplasm, targeted drug delivery

Michigan Nanotechnology Institute for Medicine and Biological Sciences, University of Michigan Medical School, BSRB, Ann Arbor, Michigan, USA

Correspondence to Andrzej Myc, PhD, MNIMBS, Rm 9346 MSRB III, University of Michigan, Ann Arbor, MI 48109, USA
Tel: +1 734 647 0052; fax: +1 734 936 2990; e-mail: myca@umich.edu

Andrzej Myc and Jolanta Kukowska-Latallo contributed equally to the study

Received 23 July 2009 **Revised form accepted** 19 October 2009

Introduction

Traditional anticancer chemotherapy uses drugs that have low functional specificity for cancer cells [1]. As a result, anticancer drugs generally have relatively small therapeutic indices, which lead to considerable nonspecific toxicity. Thus, there is a great need for anticancer drugs that specifically target cancer cells while leaving normal tissue intact.

Several approaches have been explored in an attempt to achieve site-specific chemotherapy, including localized drug administration [2], antibody-mediated targeting [3], and exploitation in the vascular structure and lymphatic drainage of solid tumors through the enhanced permeation and retention effect [4]. A large range of nano-carriers and macromolecules have been evaluated for their potential to enhance the biodistribution of chemotherapeutics to solid tumors [4–8].

Recently, a large number of applications have been found for hyperbranched polymers and dendrimers in delivering drugs and genetic materials into cells [9–19]. Compared with conventional polymers, dendrimers have structural and functional advantages emanating from their precise architecture and low polydispersity, which are synthesized in a layer-by-layer manner (called generation) around a core unit, resulting in a high level of control over size, branching points, and surface functionality [5]. The ability to tailor dendrimer properties to therapeutic needs makes them ideal carriers for small molecules such as drugs and biomolecules. Dendrimers have nanoscale container and nano-scaffolding properties and are biocompatible [5,20–25].

Conjugation of methotrexate (MTX) and folic acid (FA) to hydrazide-terminated dendrimers revealed that MTX and FA can be coupled to the dendrimer with conjugation ratios of 4.7 and 12.6, respectively [16]. In another study a 2.5 and 3-generation Poly(amido amine) dendrimers (PAMAM) dendrimer was used for the synthesis of an anticancer drug containing MTX. The conjugates increased the sensitivity of drug-resistant cell lines as compared with free MTX [26]. We have recently reported dendrimer-based drug conjugates that target cancer cells through the folate receptors [18,27–31], prostate-specific membrane antigen [32], Her2/neu [33], and $\alpha\upsilon\beta3$ integrins [34]. For the 'targeted' drug delivery agents to be useful for clinical application, the compounds have to consistently show specific killing of the targeted cells. Therefore, measuring the effect of anticancer agents on the growth and survival of neoplastic cell populations *in vitro* is critical in the preclinical evaluation of the therapeutics [35,36]. Recently, we have evaluated several lots of generation 5 (G5)-FA-MTX conjugate that target MTX to KB cells through the folate receptor and have found them preferentially cytotoxic to KB cells *in vitro* [31]. In this study, we extended the evaluation of the targeted nanotherapeutic by examining its effectiveness in an artificial heterogeneous tumor (AHT) in-vivo model [37,38]. This AHT, which consists of cells from the human epithelial KB cell line,

0959-4973 © 2010 Wolters Kluwer Health | Lippincott Williams & Wilkins DOI: 10.1097/CAD.0b013e328334560f

which overexpresses the folate receptor, and the human breast adenocarcinoma, SK-BR-3, cell line allows further confirmation of the targeting specificity and efficacy of a dendrimer-based nanotherapeutic.

Materials and methods

Materials

G5 and 7 nonacetylated dendrimers (G5-PAMAM and G7-PAMAM) were synthesized at M-NIMBS, University of Michigan, as described earlier [28,39]. The G7-PAMAM was used as a transfecting agent in the transfection of KB and SK-BR-3 cells with green fluorescent protein (GFP) and red fluorescent protein (RFP) plasmid DNA, respectively [40]. The plasmids pDsRed1-N1 and pAcGFP1-C1, which constitutively express red and green fluorescent proteins, respectively, under control of a $P_{CMV\ IE}$ promoter, were purchased from Clontech (Mountain View, California, USA).

The G5-PAMAM partially acetylated dendrimers were used to synthesize nanotherapeutics conjugated with FA and MTX [28,30]. The G5-PAMAM onto which four FA and 10 MTX molecules were attached (Lot # 123–34), was manufactured by Cambrex Corporation (East Rutherford, New Jersey). Free MTX was purchased from Sigma (St. Louis, Missouri, USA).

Cell cultures

The KB, a human epithelial cancer cell line (ATCC, Manassas, Virginia, USA), overexpresses the folate receptor, especially when grown in a medium with a low concentration of FA [41]. The KB cells were grown as a monolayer cell culture at 37°C and 5% CO_2 in either folic acid-deficient or complete (with 2.27 μmol/l FA) RPMI 1640 medium supplemented with penicillin (100 U/ml), streptomycin (100 μg/ml), and 10% heat-inactivated FBS. The SK-BR-3, a human breast adenocarcinoma cell line (ATCC), was maintained in McCoy's 5a medium supplemented with 10% heat-activated FBS, penicillin (100 U/ml), streptomycin (100 μg/ml), and 2 μmol/l L-glutamine.

To perform the coculture experiments, KB-GFP and SK-BR-3-RFP cells were mixed and grown to compare the growth rate of the two cell lines. The estimated doubling times for the KB-GFP and SK-BR-3-RFP cells were 24.8 ± 2.0 and 48.0 ± 7.3 h, respectively. To study the cytotoxic effect of the G5-FA-MTX conjugate in the coculture assay, 1×10^4 KB and 4×10^4 SK-BR-3 were mixed and seeded per well of a 12-well plate (0.5 ml/well). Twenty-four hours later the cells were treated with increasing concentrations of the G5-FA-MTX conjugate in complete or FA-deficient RPMI medium for 48–96 h and were analyzed using flow cytometry.

Transfection of KB and SK-BR-3 cells

Cell transfection was performed as described earlier [42]. Briefly, KB and SK-BR-3 cells were plated in 6-well plates 18 h before transfection to achieve 60–70% confluency. G7-PAMAM and either pDsRed1-N1 or pAcGFP1-C1 DNA were mixed to form a dendrimer/DNA complex for SKBR-3 or KB cells, respectively. The complex made with 1 μg of DNA and 6.5 μg of dendrimer was mixed with water and then allowed to form for 15 min at room temperature. The cells were washed with a serum-free medium, and 30 μl of the complex (1 μg DNA per well) was added to each well in 0.5 ml of the serum-free medium and incubated for 3 h at 37°C, 5% CO_2. The medium containing the complex was then replaced with complete growth medium. The cells remained in culture for 24 h before the selection of plasmid-transfected cells, using G418 (200 μg/ml). Single clones of stable transfectants were established by growing cells in a selective medium and cloning them using the limiting dilution technique. The expression of the reporter gene was analyzed using fluorescence microscopy and flow cytometry.

Quantitative PCR analysis

The following primers for the 500 bp fragment of the FBP α gene-spanning intron sequences were used for PCR. The primer set used was 5′-GCATGTGAATGCAGGTGA-3′ and 5′-ACGGGCTTTCTAGGCAA-3′. The primer set used for the 500 bp fragment of the housekeeping gene (HKG), β-actin was 5′-TGCATCCTGTCGGCAA-3′ and 5′-TACGCCTCTGgCCTA-3′. All primers were prepared by *idtdna.com*. Total RNA was isolated from cell lines using Tri Reagent (MRC, Cincinnati, Ohio, USA). cDNA synthesis (reverse transcription) was carried out with 1 μg of total RNA in the reaction containing 5 mmol/l $MgCl_2$, 500 μmol/l of each dNTP, 2.5 μmol/l random hexamer primers, and 2.5 U/μl of reverse transcriptase (Superscript II RT, Invitrogen, Carlsbad, California, USA). Total RNA was reverse transcribed for 10 min at 25°C, 50 min at 42°C, and for 15 min at 70°C. After reverse transcription the samples were incubated with RNase H (0.1 U/μl) for 20 min at 37°C to remove the remaining RNA template. Quantitative PCR was performed using 0.001–0.1 μg of cDNA, 0.3 μmol/l of each primer, 1.25 U of Platinum Taq (Invitrogen), 0.2 mmol/l of each dNTP, 1.5 mmol/l $MgCl_2$, 0.5X SYBR Green (Invitrogen), 0.2 mg/ml of bovine serum albumin Fraction V, 150 mmol/l trehalose, and 0.2% Tween 20. PCR was carried out in a Cepheid SmartCycler (Sunnyvale, California, USA) in a total volume of 25 μl, incubated at 95°C for 2 min, followed by 45 cycles of denaturation at 95°C (15 s), annealing at 66°C (15 s) and extension at 72°C (25 s). Finally, the melt curve of the product was made at 60–95°C at 0.2°C/s. Relative fold change ($2^{-\Delta Ct}$) was calculated by normalizing the expression level of the FBP gene of interest (GOI) to the β-actin HKG. The expression levels of the two genes were divided as follows:

$$2^{-\mathrm{Ct(GOI)}} / 2^{-\mathrm{Ct(HKG)}} = 2^{-[\mathrm{Ct(GOI)} - \mathrm{Ct(HKG)}]} = 2^{-\Delta \mathrm{Ct}}$$

Determining the 50% cytotoxic dose of methotrexate using the XTT assay

The cytotoxic dose of MTX resulting in a 50% reduction of the viable cells (CD_{50}) was determined by XTT assay for both cell lines. CD_{50} was calculated by the extrapolation of the corresponding dose–response curve on a log-linear plot, using the portions of the curve that transected the 50% response point. The CD_{50} (MTX) was 37 nmol/l for KB and 33 nmol/l for SK-BR-3 cells, respectively, indicating that these two cell lines are equally sensitive to the drug.

Flow cytometry analysis

At the end of the coculture assay, the cells were harvested, resuspended in PBS containing 0.1% bovine serum albumin, and acquired on a Beckman–Coulter EPICS-XL MCL flow cytometer. Collected data were analyzed using Expo32 software (Beckman-Coulter, Miami, Florida, USA). Dead cells were stained with propidium iodide dye as described earlier [43]. To estimate the absolute number of cells in each coculture, equal volume samples of the coculture were acquired and analyzed using flow cytometry.

Recipient animal and tumor model

A heterogeneous xenograft tumor model was established in NOD C.B-17 SCID mice, using tumor cells as described earlier [37]. Briefly, 5–6-week-old FOX CHASE SCID (C.B-17/IcrCrl-scidBR) female mice were purchased from the Charles River Laboratories (Wilmington, Massachusetts, USA) and housed in a specific, pathogen-free animal facility at the University of Michigan Health System in accordance with the regulations of the University's Committee on the Use and Care of Animals as well as with federal guidelines, including the Principles of Laboratory Animal Care. Animals were fed *ad libitum* with Laboratory Autoclavable Rodent Diet 5010 (PMI Nutrition International, St. Louis, Missouri, USA). The food was changed to a folate-deficient diet (TestDiet, Richmond, Indiana, USA) 7 days before tumor implantation [27]. AHTs were established on both flanks of the mice using two human cell lines, each one expressing a different fluorescent protein. Subcutaneous injection of 10^6 of cells of each clone (green KB-GFP and red SK-BR-3-RFP) was performed in a volume of 0.2 ml of PBS in both flanks of the mice. Subcutaneous tumor nodules appeared 7 days postimplantation. Subcutaneous injections of either the nanotherapeutic (G5-FA-MTX) or free MTX in 0.2 ml of saline were started 7 days after implantation. The mice were given equimolar concentrations of MTX or the nanotherapeutic (13.7 nmoles) per subcutaneous injection. The formula chosen to compute tumor volume was for a standard volume of an ellipsoid, where $V=4/3;\pi$ (½ length × ½ width × ½ depth) as described elsewhere [44,45]. With the assumption that width equals depth and π equals 3, the formula used was $V=½ \times \text{length} \times \text{width}^2$.

Statistics

All data are expressed as a mean of values and ± SEs. Differences between the experimental groups and the control group were tested using the analysis of variance test.

Results

PCR analysis of the α-FBP receptor on KB and SK-BR-2 cells

The receptor status of cell lines was confirmed by quantitative RT-PCR and revealed the expression of folate binding protein mRNA in the KB-GFP cell clones and the KB parental cell line and the absence of the specific message in the SK-BR-3-RFP cell clones (Table 1).

In-vitro evaluation of G5-FA-methotrexate nanotherapeutic cytotoxicity against KB and SK-BR-3 cells

To evaluate the G5-FA-MTX nanotherapeutic, the coculture technique was applied as described by us earlier [31]. Using the coculture assay, we could calculate the absolute number of cells in both populations, which offers insightful information on the interaction of the tested anticancer drugs with both targeted and nontargeted (bystander) cells. The KB-GFP and nonfluorescent SK-BR-3 cells were cocultured together 24 h before the treatment. Afterward the cells were treated with the G5-FA-MTX nanotherapeutic for 48 h. The cells were harvested, stained with propidium iodide to exclude dead cells, and analyzed using flow cytometry. Figure 1 represents a dot plot of the cocultured control and treated cells. As shown in Fig. 1b, the G5-FA-MTX nanotherapeutic preferentially reduced the viability of the KB-GFP cells, compared with the SK-BR-3 cells, which do not express the α-FBP receptor and compared with the untreated control culture (Fig. 1a). The preferential cytotoxic effect of the nanotherapeutic on the KB-GFP cells cocultured with SK-BR-3 cells after 48-h treatment is shown in Fig. 1. It was statistically significant in a broad range of nanotherapeutic concentrations; however, in the higher concentrations it was also cytotoxic to some extent to SK-BR-3 cells. The cytotoxic effect was abolished when the cells were cultured in a medium containing high levels of FA (2.27 μmol/l), indicating competition for α-FBP receptors between FA and the G5-FA-MTX nanotherapeutic and the inability of the conjugate to kill KB cells in an excess of FA (Fig. 2a vs. Fig. 2b). The cytotoxic effect of the nanotherapeutic was dose-dependent and time-dependent.

Evaluation of the G5-FA-methotrexate nanotherapeutic *in vivo*

Experimental animals were injected subcutaneously in both flanks with a mixture of 10^6 of KB-GFP (green fluorescent) and 10^6 SK-BR-3-RFP (red fluorescent) cells. Seven days after the heterogeneous tumor implantation, the mice were treated by subcutaneous

Fig. 1

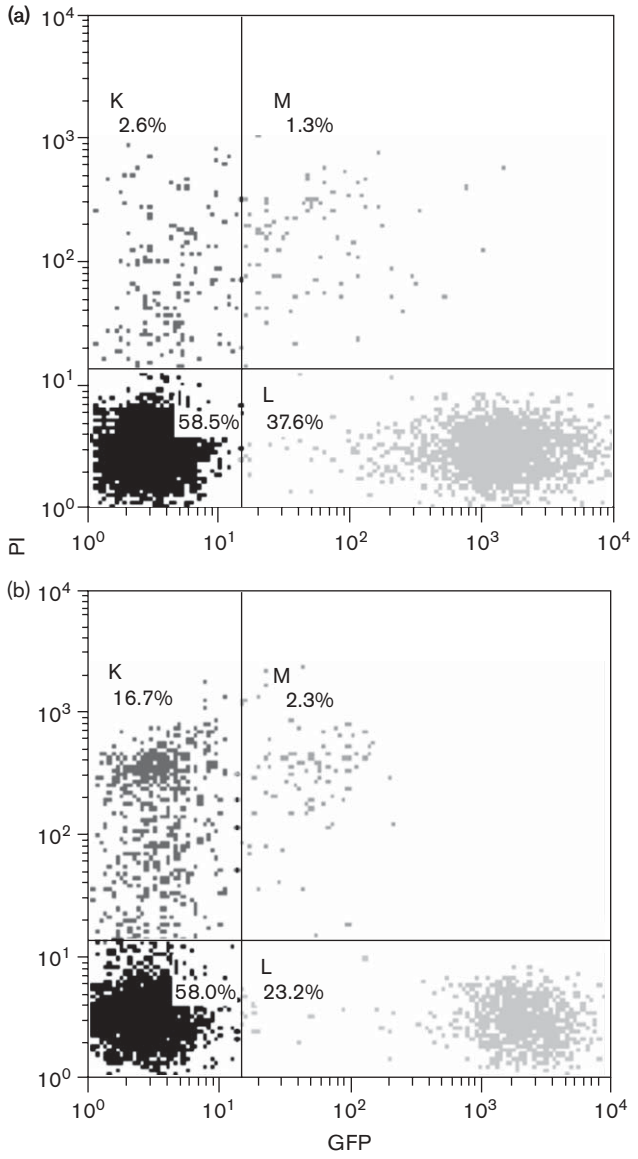

Flow cytometry analysis of the coculture of KB-GFP (green fluorescent, quadrant L) and SK-BR-3 (nonfluorescent, quadrant I) control cells (a) and nanotherapeutic (40 nmol/l G5-FA-MTX) treated cells (b) after 72-h incubation. In the control coculture, 4606 (37.6%) KB cells (green fluorescence, quadrant L), 7165 (58.5%) SK-BR-3 cells (nonfluorescent, quadrant I) and 317 (2.6%) dead cells [stained with propidium iodide (PI), red fluorescence, quadrant 1] were acquired. In the treated coculture, 1782 (23.2%) KB cells (green fluorescence, quadrant L), 4446 (58.0%) SK-BR-3 cells (nonfluorescent, quadrant I), and 1284 (16.7%) dead cells (stained with PI, red fluorescence, quadrant K) were acquired. To estimate the absolute number of cells in each coculture, equal volume samples of the coculture were acquired and analyzed using flow cytometry.

injection of either the G5-FA-MTX or free MTX in 0.2 ml of saline, or saline alone. The injections were given twice a week for 4 weeks. The tumor size was measured on days 11 and 32 after implantation. Both cell clones contributed to tumor size, resulting in more frequent green fluorescent (KB-GFP) than red fluorescent (SK-BR-3-RFP) cells (data not shown). As shown in Fig. 3, significant inhibition of tumor growth was observed on days 11 and 32 in the animals treated with G5-FA-MTX, compared with the saline-treated animals ($P < 0.04$). Treatment with free MTX inhibited tumor growth to some extent, compared with the inhibition of tumor growth in the saline-treated animals. There were also fewer targeted than non-targeted cells in the tumor post-treatment (Table 2).

Discussion

Current cancer chemotherapies are dose-limited by side effects resulting from the cytotoxicity of normal and tumor cells. To overcome this problem, significant efforts have been made to target anticancer drugs exclusively to neoplastic cells [46]. This approach, however, has had limited success because of the absence of high-affinity targeting ligands for cancer cells. In addition, many targeted materials exceed the size required to escape the vasculature (< 50 nm) and interact with individual cells. Therefore, having a targeting therapeutic that is small enough to reach tumor cells and internalize with specificity is desirable.

Dendrimer-based drug delivery molecules have several potential advantages. Dendrimers are comparable in size to proteins and small enough (< 7.0 nm diameter) to escape the vasculature and target tumor cells, while remaining below the renal filtration threshold. Dendrimers are not retained in the filter organs and therefore do not need to undergo hepatic metabolism. The G5 PAMAM dendrimer is stable, nonimmunogenic [47,48; and J. Kukowska-Latallo, personal communication], and on average contains 110 primary amines. These amines provide ample reactive sites for the conjugation of the complex drug delivery systems and multiple chemical moieties, such as radiopharmaceuticals, dyes, and contrast agents. Dendrimers can also be chemically synthesized in large quantities, allowing for the potential scale-up of the technology.

In our earlier report we documented for the first time tumor cell-targeted delivery and the therapeutic effect of dendrimer–drug conjugates *in vivo* [27]. We showed a significant enhancement in the therapeutic index of a targeted dendrimer – drug conjugate over a free drug. This enhancement may have been due to a decrease in nonspecific toxicity, an increase in drug effectiveness, or both. Uptake of the targeted but not the control dendrimer conjugate can be partially inhibited in the tumor by an earlier administration of an excess of free FA [27]. This is consistent with the in-vitro binding and internalization studies of the multifunctional dendrimer conjugate [18].

Although chemical and functional analysis of the G5-FA-MTX nanotherapeutic confirmed its structure and biological properties, there is still a need for a simple and dependable method to evaluate the large-scale synthesized

Fig. 2

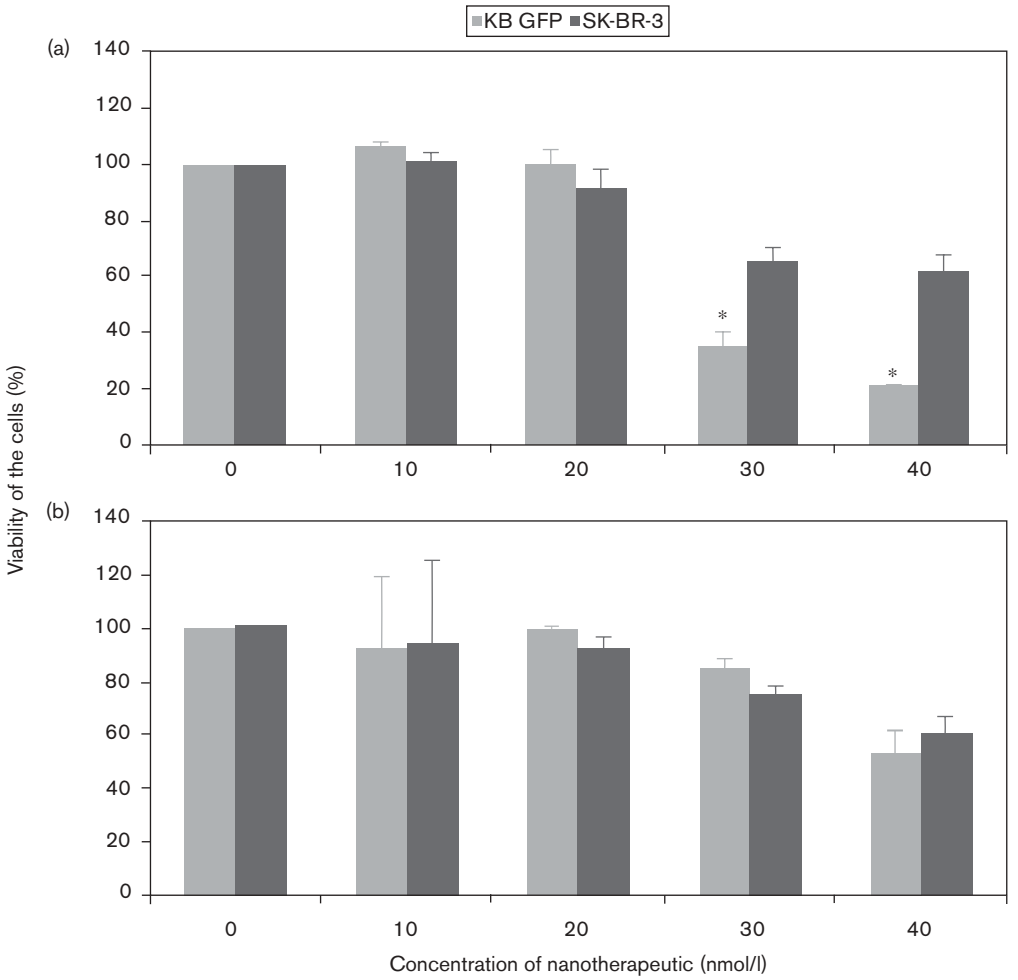

In-vitro cytotoxicity of the G5- folic acid (FA)-methotrexate (MTX) nanotherapeutic against KB cells. The KB-GFP (green fluorescent) and SK-BR-3 (nonfluorescent) cells were treated with different concentrations of G5-FA-MTX conjugate for 48 h in medium without FA (a) and in medium containing 2.27 μmol/l FA (b). The nanotherapeutic-treated KB cells were significantly reduced in number, compared with the untreated KB cells and treated SK-BR-3 cells ($P<0.05$) (a). The presence of 2.27 μmol/l FA in the medium abolished the cytotoxic effect of the conjugate (b).

nanotherapeutics *in vivo*. In our earlier study, we applied a coculture assay to test the effect of the drug on targeted and non-targeted cell populations simultaneously [31]. We found that this method better assesses preferential cytotoxicity towards targeted cells than the single cell-type cultures used in XTT, clonogenic, and other types of cytotoxicity assays. In this study, in addition to the coculture assay, we extended preclinical evaluation and employed an artificial heterogeneous xenograft tumor model in NOD C.B-17 SCID mice to evaluate the new generation of nanotherapeutics. The tumor model applied here is capable of assessing the preferential toxicity of a nanotherapeutic against targeted cells (KB) *in vivo*. We observed tumor growth inhibition in mice treated with the nanotherapeutic, compared with mice treated with either free MTX or saline. Tumor growth inhibition after nanotherapeutic treatment, although significant, was not as dramatic as observed in our earlier study, in which we used a homogeneous xenograft tumor model consisting of a single targeted cell line (KB) and an intravenous delivery route [27]. In this study the AHT model consisting of fluorescent KB and SK-RB-3 cells allowed for direct examination of a relative number of targeted and non-targeted cells in the tumor using flow cytometry. The results showed that the targeted nanodevice preferentially killed KB-GFP cells. Indeed, despite the two-fold difference in doubling time (22.5 and 42.5 h for KB-GFP and SK-BR-3-RFP, respectively), there were fewer targeted than non-targeted cells in the tumor posttreatment (Fig. 3 and Table 2). The AHT used in this study enabled us to compare the targeting efficiency of the dendrimer–drug nanoconjugate to targeted (KB-GFP) and nontargeted (SKBR-3-RFP) cells. With the recent development of vectors expressing fluorescent proteins, which allow for the easy identification of different cell populations, a more sophisticated

Fig. 3

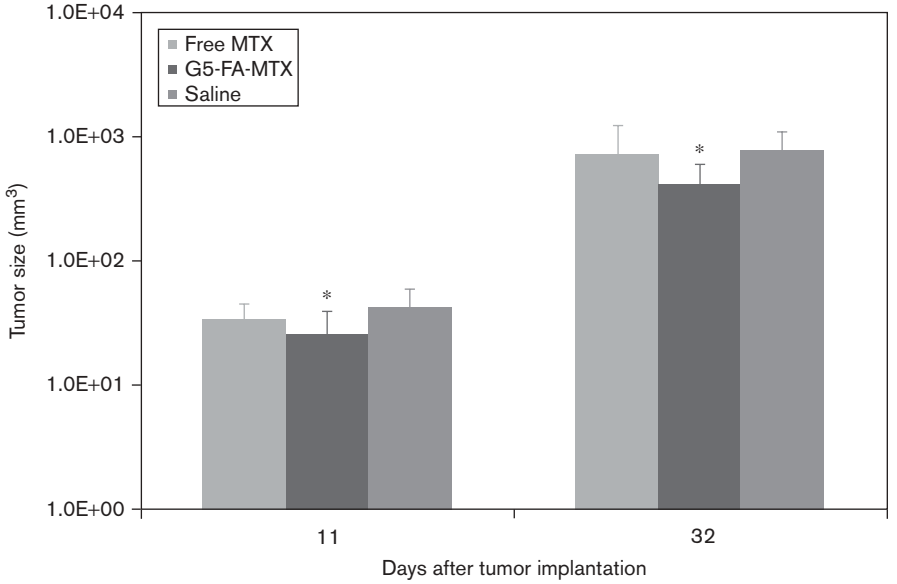

Inhibition of tumor growth in SCID mice. Mice were inoculated subcutaneously with a mixture (1 : 1) of KB-GFP and SK-BR-3-RFP; 10^6 cells of each cell line in 0.2 ml of PBS in each flank. Subcutaneous injections of equimolar concentrations (13.7 nmol) of the nanotherapeutic (G5-folic acid (FA)-methotrexate (MTX) lot#123–34) or free MTX in 0.2 ml of saline were started 7 days after implantation. The mice were treated twice a week for 4 weeks. Tumor volumes (mm^3) were measured at 11 and 32 days after implantation ($P<0.04$).

Table 1 PCR analysis of α-FBP receptor on KB and SK-BR-3 cells

Cell lines	Fold change of FOLR1 (α-FBP) versus β-actin
KB	23.6
KB GFP	63.5
SK-BR-3 RFP	0.1

Table 2 Number of KB (green) and SK-BR-3 (red) cells harvested from tumors of control animals and animals treated with MTX or nanotherapeutic[a]

		KB GFP		SK-BR-3 RFP	
	N	Average	SD	Average	SD
Saline	6	1748	377.7	222	127.1
MTX	6	1590	626.6	320	137.7
G5-FA-MTX	6	1273*	291.9	217	44.1

MTX, methotrexate; SD, standard deviation.
[a]Cells were released from tumors as described in Material and methods and fixed. Then 10 000 cells from each tumors sample were analyzed on flow cytometry.
*$P<0.04$.

GRF, green flourescent protein; RFF, red flourescent protein.

heterogeneous tumor model can be designed to supply more detailed information on the interaction of the targeted nanotherapeutics with cell populations having different growth rates *in vivo*.

Conclusion

In this report, we used a coculture assay and an artificial heterogeneous xenograft tumor model in NOD C.B-17 SCID mice to evaluate a new generation of nanotherapeutics both *in vitro* and *in vivo*. Data obtained from both studies showed preferential killing of targeted cells by the nanotherapeutic. These findings confirm the specificity of the G5-FA-MTX nanotherapeutic and predict its clinical applicability as a potential drug for targeted anticancer therapy.

Acknowledgements

This study has been funded in whole or in part with federal funds from the National Cancer Institute, National Institutes of Health, under award 1 R01 CA119409. The authors wish to thank Patricia Gold and Dr Pascale Leroueil for editorial help in preparing the manuscript for submission and Lauren Zetts for purification of plasmids.

References

1 Malhotra V, Perry MC. Classical chemotherapy: mechanisms, toxicities and the therapeutic window. *Cancer Biol Ther* 2003; **2** (**4 Suppl 1**):S2–S4.
2 Read TA, Thorsen F, Bjerkvig R. Localised delivery of therapeutic agents to CNS malignancies: old and new approaches. *Curr Pharm Biotechnol* 2002; **3**:257–273.
3 Albrecht H, DeNardo SJ. Recombinant antibodies: from the laboratory to the clinic. *Cancer Biother Radiopharm* 2006; **21**:285–304.
4 Iyer AK, Khaled G, Fang J, Maeda H. Exploiting the enhanced permeability and retention effect for tumor targeting. *Drug Discov Today* 2006; **11**:812–818.
5 Gillies ER, Frechet JM. Dendrimers and dendritic polymers in drug delivery. *Drug Discov Today* 2005; **10**:35–43.
6 Pinto RC, Neufeld RJ, Ribeiro AJ, Veiga F. Nanoencapsulation II. Biomedical applications and current status of peptide and protein nanoparticulate delivery systems. *Nanomedicine* 2006; **2**:53–65.

7 Portney NG, Ozkan M. Nano-oncology: drug delivery, imaging, and sensing. *Anal Bioanal Chem* 2006; **384**:620–630.
8 Kaminskas LM, Kelly BD, McLeod VM, Boyd BJ, Krippner GY, Williams ED, Porter CJ. Pharmacokinetics and tumor disposition of PEGylated, methotrexate conjugated poly-l-lysine dendrimers. *Mol Pharm* 2009; **6**:1190–1204.
9 Cloninger MJ. Biological applications of dendrimers. *Curr Opin Chem Biol* 2002; **6**:742–748.
10 Frey H, Haag R. Dendritic polyglycerol: a new versatile biocompatible-material. *J Biotechnol* 2002; **90**:257–267.
11 Godbey WT, Wu KK, Mikos AG. Poly(ethylenimine) and its role in gene delivery. *J Control Release* 1999; **60**:149–160.
12 Kannan S, Kolhe P, Raykova V, Glibatec M, Kannan RM, Lieh-Lai M, Bassett D. Dynamics of cellular entry and drug delivery by dendritic polymers into human lung epithelial carcinoma cells. *J Biomater Sci Polym Ed* 2004; **15**:311–330.
13 Khandare J, Kolhe P, Pillai O, Kannan S, Lieh-Lai M, Kannan RM. Synthesis, cellular transport, and activity of polyamidoamine dendrimer-methylprednisolone conjugates. *Bioconjug Chem* 2005; **16**:330–337.
14 Kolhe P, Khandare J, Pillai O, Kannan S, Lieh-Lai M, Kannan R. Hyperbranched polymer-drug conjugates with high drug payload for enhanced cellular delivery. *Pharm Res* 2004; **21**:2185–2195.
15 Kolhe P, Misra E, Kannan RM, Kannan S, Lieh-Lai M. Drug complexation, *in vitro* release and cellular entry of dendrimers and hyperbranched polymers. *Int J Pharm* 2003; **259**:143–160.
16 Kono K, Liu M, Frechet JM. Design of dendritic macromolecules containing folate or methotrexate residues. *Bioconjug Chem* 1999; **10**:1115–1121.
17 Ooya T, Lee J, Park K. Effects of ethylene glycol-based graft, star-shaped, and dendritic polymers on solubilization and controlled release of paclitaxel. *J Control Release* 2003; **93**:121–127.
18 Thomas TP, Majoros IJ, Kotlyar A, Kukowska-Latallo JF, Bielinska A, Myc A, Baker JR Jr. Targeting and inhibition of cell growth by an engineered dendritic nanodevice. *J Med Chem* 2005; **48**:3729–3735.
19 Wiwattanapatapee R, Carreno-Gomez B, Malik N, Duncan R. Anionic PAMAM dendrimers rapidly cross adult rat intestine *in vitro*: a potential oral delivery system? *Pharm Res* 2000; **17**:991–998.
20 Cheng Y, Wang J, Rao T, He X, Xu T. Pharmaceutical applications of dendrimers: promising nanocarriers for drug delivery. *Front Biosci* 2008; **13**:1447–1471.
21 Gupta U, Agashe HB, Asthana A, Jain NK. Dendrimers: novel polymeric nanoarchitectures for solubility enhancement. *Biomacromolecules* 2006; **7**:649–658.
22 Li Y, Cheng Y, Xu T. Design, synthesis and potent pharmaceutical applications of glycodendrimers: a mini review. *Curr Drug Discov Technol* 2007; **4**:246–254.
23 Svenson S. Dendrimers as versatile platform in drug delivery applications. *Eur J Pharm Biopharm* 2009; **71**:445–462.
24 Svenson S, Chauhan AS. Dendrimers for enhanced drug solubilization. *Nanomed* 2008; **3**:679–702.
25 Svenson S, Tomalia DA. Dendrimers in biomedical applications – reflections on the field. *Adv Drug Deliv Rev* 2005; **57**:2106–2129.
26 Gurdag S, Khandare J, Stapels S, Matherly LH, Kannan RM. Activity of dendrimer-methotrexate conjugates on methotrexate-sensitive and -resistant cell lines. *Bioconjug Chem* 2006; **17**:275–283.
27 Kukowska-Latallo JF, Candido KA, Cao Z, Nigavekar SS, Majoros IJ, Thomas TP, *et al*. Nanoparticle targeting of anticancer drug improves therapeutic response in animal model of human epithelial cancer. *Cancer Res* 2005; **65**:5317–5324.
28 Majoros IJ, Thomas TP, Mehta CB, Baker JR Jr. Poly(amidoamine) dendrimer-based multifunctional engineered nanodevice for cancer therapy. *J Med Chem* 2005; **48**:5892–5899.
29 Patri AK, Majoros IJ, Baker JR. Dendritic polymer macromolecular carriers for drug delivery. *Curr Opin Chem Biol* 2002; **6**:466–471.
30 Quintana A, Raczka E, Piehler L, Lee I, Myc A, Majoros I, *et al*. Design and function of a dendrimer-based therapeutic nanodevice targeted to tumor cells through the folate receptor. *Pharm Res* 2002; **19**:1310–1316.
31 Myc A, Douce TB, Ahuja N, Kotlyar A, Kukowska-Latallo J, Thomas TP, Baker JR Jr. Preclinical antitumor efficacy evaluation of dendrimer-based methotrexate conjugates. *Anticancer Drugs* 2008; **19**:143–149.
32 Patri AK, Myc A, Beals J, Thomas TP, Bander NH, Baker JR Jr. Synthesis and *in vitro* testing of J591 antibody-dendrimer conjugates for targeted prostate cancer therapy. *Bioconjug Chem* 2004; **15**:1174–1181.
33 Shukla R, Thomas TP, Peters JL, Desai AM, Kukowska-Latallo J, Patri AK, *et al*. HER2 specific tumor targeting with dendrimer conjugated anti-HER2 mAb. *Bioconjug Chem* 2006; **17**:1109–1115.
34 Shukla R, Thomas TP, Peters J, Kotlyar A, Myc A, Baker JR Jr. Tumor angiogenic vasculature targeting with PAMAM dendrimer–RGD conjugates. *Chem Commun* 2005; **46**:5739–5741.
35 Bosanquet AG, Burlton AR, Bell PB, Harris AL. Ex vivo cytotoxic drug evaluation by DiSC assay to expedite identification of clinical targets: results with 8-chloro-cAMP. *Br J Cancer* 1997; **76**:511–518.
36 Weinstein JN, Myers TG, O'Connor PM, Friend SH, Fornace AJ Jr, Kohn KW, *et al*. An information-intensive approach to the molecular pharmacology of cancer. *Science* 1997; **275**:343–349.
37 Leith JT, Michelson S, Faulkner LE, Bliven SF. Growth properties of artificial heterogeneous human colon tumors. *Cancer Res* 1987; **47**:1045–1051.
38 Leith JT, Faulkner LE, Bliven SF, Michelson S. Compositional stability of artificial heterogeneous tumors *in vivo*: use of mitomycin C as a cytotoxic probe. *Cancer Res* 1988; **48**:2669–2673.
39 Shi X, Majoros IJ, Patri AK, Bi X, Islam MT, Desai A, *et al*. Molecular heterogeneity analysis of poly(amidoamine) dendrimer-based mono- and multifunctional nanodevices by capillary electrophoresis. *Analyst* 2006; **131**:374–381.
40 Bielinska AU, Chen C, Johnson J, Baker JR Jr. DNA complexing with polyamidoamine dendrimers: implications for transfection. *Bioconjug Chem* 1999; **10**:843–850.
41 Antony AC, Kane MA, Portillo RM, Elwood PC, Kolhouse JF. Studies of the role of a particulate folate-binding protein in the uptake of 5-methyltetrahydrofolate by cultured human KB cells. *J Biol Chem* 1985; **260**:14911–14917.
42 Kukowska-Latallo JF, Bielinska AU, Johnson J, Spindler R, Tomalia DA, Baker JR Jr. Efficient transfer of genetic material into mammalian cells using Starburst polyamidoamine dendrimers. *Proc Natl Acad Sci U S A* 1996; **93**:4897–4902.
43 Jacobs DB, Pipho C. Use of propidium iodide staining and flow cytometry to measure anti-mediated cytotoxicity: resolution of complement-sensitive and resistant target cells. *J Immunol Methods* 1983; **62**:101–108.
44 Euhus DM, Hudd C, LaRegina MC, Johnson FE. Tumor measurement in the nude mouse. *J Surg Oncol* 1986; **31**:229–234.
45 Tomayko MM, Reynolds CP. Determination of subcutaneous tumor size in athymic (nude) mice. *Cancer Chemother Pharmacol* 1989; **24**:148–154.
46 Leamon CP, Reddy JA. Folate-targeted chemotherapy. *Adv Drug Deliv Rev* 2004; **56**:1127–1141.
47 Eliyahu H, Barenholz Y, Domb AJ. Polymers for DNA delivery. *Molecules* 2005; **10**:34–64.
48 Tomalia DA, Reyna LA, Svenson S. Dendrimers as multi-purpose nanodevices for oncology drug delivery and diagnostic imaging. *Biochem Soc Trans* 2007; **35(Pt 1)**:61–67.